

## Six-Fold D-shaped Surface Plasmon Resonance based Photonic Crystal Fibre Sensor

Open Access

Abdosllam M. Abobaker<sup>1,\*</sup>, Suoda Chu<sup>2</sup>, K. Nakkeeran<sup>2</sup>, Sumeet S. Aphale<sup>2</sup>, P. Ramesh Babu<sup>3</sup>, K. Senthilnathan<sup>3</sup>

<sup>1</sup> Department of Communications Engineering, College of Electronic Technology, Bani Walid, Libya

<sup>2</sup> School of Engineering, Fraser Noble Building, University of Aberdeen, Aberdeen AB24 3UE, UK

<sup>3</sup> Photonics Research Laboratory, School of Advanced Sciences, VIT University, Vellore-632 014, Tamil Nadu, India

### ARTICLE INFO

### ABSTRAK

#### Article history:

Received 3 September 2019

Received in revised form 2 October 2019

Accepted 10 October 2019

Available online 5 November 2019

In this work, we design a 6-fold D-shaped photonic crystal fibre based surface plasmon resonance sensor in detail. The sensing performance of a standard 6-fold hexagonal D-shaped PCF-SPR sensor on a large analyte refractive index range from 1.33 to 1.48 was numerically investigated. The numerical results obtained from the finite element method simulations reveal the coupling relations between fundamental core mode and three surface plasmonic modes which have different electric field distributions for analytes with different refractive index (RI). Two different types of SPRs, namely, 'dielectric like' resonance with low-loss peak and 'plasmon like' resonance with high-loss peak, are also found through a critical analysis on the electric field distribution evolutions of the fibre modes. In order to reduce the negative influence from the sub-peak of the secondary SPR on the sensor's dynamic sensing range (DSR), we found that by adjusting the liquid analyte layer/analyte binding layer thickness from thick layer (1500 nm) to thin layer (500 nm), the DSR can be extended by a ratio of 44.4% from 1.33-1.41 to 1.33-1.45 at the cost of a reduced maximum sensitivity from 7900 nm/RIU to 5300 nm/RIU. Owing to the simple structure design of the proposed sensor, we envisage that this highly sensitive D-shaped PCF-SPR sensor could be developed as a versatile and competitive instrument with a large and flexible refractive index detection range.

#### Keywords:

D-shaped, Sensor, Photonic crystal Fibre, Refractive Index Sensor, Sensitivity, Surface Plasmon Resonance

Copyright © 2019 PENERBIT AKADEMIA BARU - All rights reserved

## 1. Introduction

The sensing applications based on the optical excitation and detection of the surface plasmon resonance (SPR) phenomenon have been widely studied. The fibre sensors based on SPR are proven to be a commercial-successful technology in the field of medical diagnosis, chemical detection, biochemical reaction test/recognition, food safety control, environment monitoring, etc. The high sensitivity to the change of refractive index of the medium in contact with the surface of thin metal

\* Corresponding author.

E-mail address: [almahjub11@gmail.com](mailto:almahjub11@gmail.com) (Abdosllam M. Abobaker)

film (typically gold or silver with dielectric), has been widely utilized for those sensing applications [1-3].

The SPR phenomenon is generally defined as the strong coupling between the electromagnetic wave and surface plasmon wave at the interface of dielectric and metal [4]. Then optical fibre was introduced as the dielectric medium to overcome the traditional configuration's drawbacks. Due to its design flexibility and compact in size [5], the metal coated optical fibres, as an idea alternative to the prism, have been utilized to form the excitation of surface plasmons [6-8]. Therefore, low-cost, highly integrable, miniaturization and portable optical fibre based SPR sensors have been achieved. Recently, photonic crystal fibre (PCF) is widely used as a novel class of optical fibre for different sensing purposes. The PCF-SPR based sensors are now widely studied because of their simple and compact probe designed for high sensitivity, highly robust, low-cost, fast response, label-free detection [9]. Moreover, by optimizing the structural parameters like air holes' diameters, the distance between two adjacent air holes, it is possible to enhance the sensitivity and the sensing range. The hexagonal D-shaped PCF is one of the most frequently used fibre media for common PCF-SPR sensor applications. In this paper, we numerically investigate the sensing performance of a standard 6-fold hexagonal D-shaped PCF-SPR sensor on a large analyte refractive index range from 1.33 to 1.48. A comprehensive numerical analysis based on the finite element method (FEM) is adopted.

## 2. Geometrical Structure and Numerical Analysis

The schematic of the proposed biosensor is shown in Fig. 1. It comprises of four layers of air holes arranged in a six-fold hexagonal PCF structure of air holes diameter of  $d=1.2\ \mu\text{m}$  with a solid core. The distance between two holes (pitch),  $\lambda$ , is  $2.5\ \mu\text{m}$  and the radius of the whole sensor is set as  $11\ \mu\text{m}$ . An open D-shaped analyte channel is designed at the top part of the fibre cross-section so that the analyte can be infused in the channel. The height of the D-shaped channel,  $d_a$ , is  $8\ \mu\text{m}$ . A uniform nano-scale gold metal film is deposited on the flat side-polished surface with its layer thickness of  $t_{Au}=45\ \text{nm}$  for surface plasmon polaritons generation. The liquid analyte layer thickness in the D-shaped channel is considered as  $1500\ \text{nm}$ .

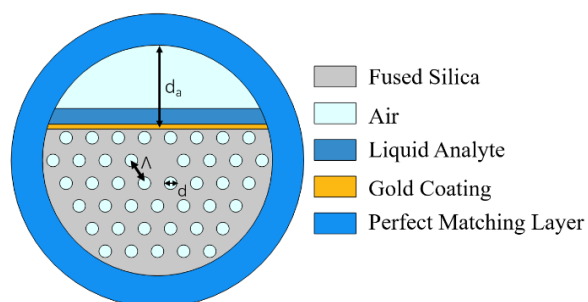
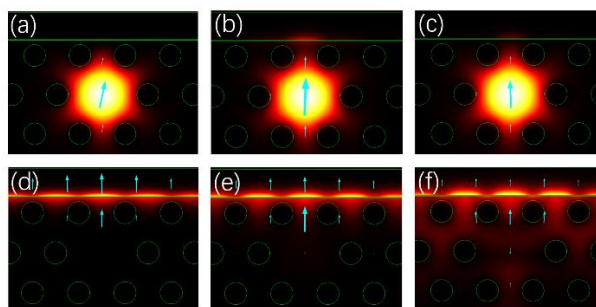


Fig. 1. Cross-section of the proposed six-fold PCF-LSPR sensor

## 3. Analysis of Modes

It is well known that the surface plasmon mode (PM) is generated and coupled with the main core-guided fundamental mode (FM) at particular resonant wavelength [10]. In other words, it means that there is a light energy transfer between those two modes. At the resonance wavelength, the loss spectra of the majority of fibre-based SPR sensors exhibit single-resonance-peak characteristic with a sharp and deep resonance peak [11].



**Fig. 2.** Light distributions in the cross-section of D-shaped PCF-SPR sensor for different wavelengths for the analyte RI of  $n_a=1.38$ . (a) and (d) are the FM and PM at 600 nm (shorter wavelength with respect to the resonance). (b) and (e) are the FM and PM at resonant wavelength of 690 nm. (c) and (f) are the FM and PM at 770 nm (longer wavelength with respect to the resonance). The arrows indicate the direction of the electric field

The formation of the PM is shown in Figs. 2. The refractive index of the liquid analyte is considered as  $n_a=1.38$ . Figures 2 illustrate both the distribution of the light energy flow of the FM [Figs. 2 (a), 2 (b) and 2 (c)] and the PM [Figs. 2 (d), 2 (e) and 2 (f)] of the proposed sensor at 600 nm. Here, the arrows indicate the direction of the electric field. Figures 2 (d), 2 (e) and 2 (f) show the formation of the PM for all three wavelengths, viz., shorter, equal and longer with respect to the resonant wavelength. In Figs. 2 (b), a weak surface plasmon resonance can be observed at the inference between the thin gold film and the dielectric (optical fibre). From Figs. 2 (a) to 2 (c), it is clear to show a full process of SPR.

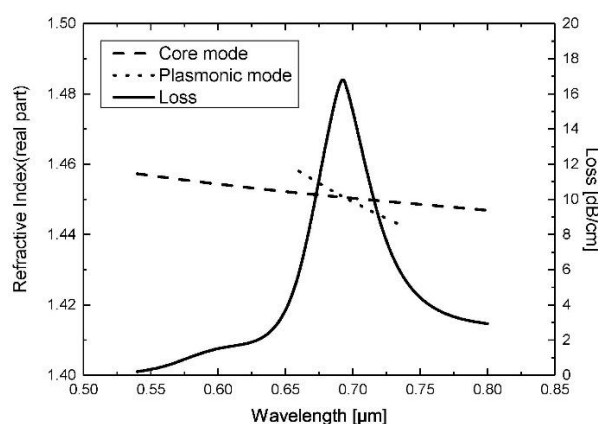


**Fig. 3.** The confinement loss, dispersion relations of FM and PM of the D-shaped hexagonal PCF-SPR sensor for an analyte RI of 1.38

Figure 3 shows the confinement loss spectrum (solid curve), dispersion relations of the FM (dashed curve) and PM (dot-dashed curve) for the D-shaped hexagonal PCF-SPR sensor when the RI of an analyte is 1.38. As it is illustrated in Fig. 3, a sharp and deep single resonance peak has been obtained by proposed sensor for  $n_a=1.38$  at the resonance wavelength of 690 nm.

However, for higher refractive index analyte range of 1.46, two resonance peaks are found in the confinement loss spectrum at their resonance wavelengths of 1337.5 nm and 1515 nm as shown in Fig. 4.

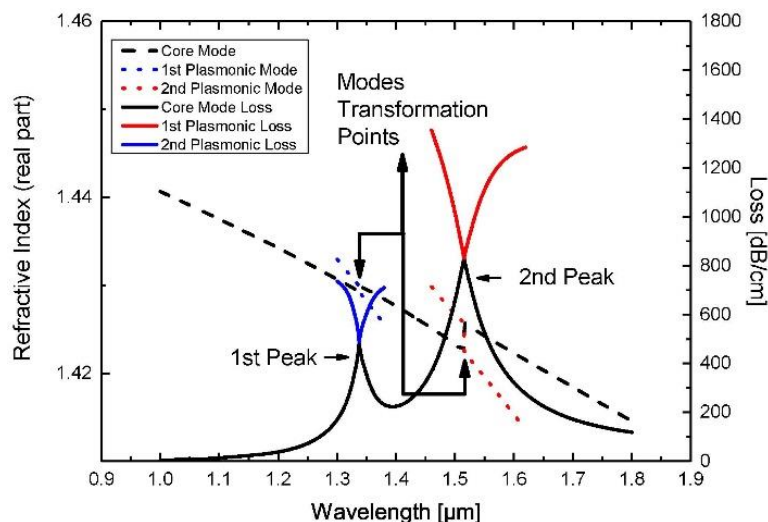


**Fig. 4.** The confinement loss, dispersion relations of FM and PM of the D-shaped hexagonal PCF-SPR sensor for analyte RI  $n_a=1.46$

For a large range of analyte RI, there are two different types of SPRs for the proposed D-shaped hexagonal PCF-SPR sensor, the 'dielectric-like' SPR and the 'plasmon-like' SPR, respectively. In literature, they are also named as 'incomplete coupling' and 'complete coupling' [12-14]. Therefore, the phase matching conditions for them are found to be different with each other as well. For lower RI of analyte, as its resonance wavelength is usually located at shorter wavelength region, the 'dielectric-like' SPR will occur with the phase matching condition of the equality between the real parts of effective refractive indices ( $n_{eff}$ ) for FM and the PM at upper boundary of gold film surface. On the other hand, for higher RI analytes, as their resonance wavelengths are usually located at longer wavelength region, the 'plasmon-like' SPR will occur at the surface of gold film.

#### 4. Sensing Performance

In the sensing process, to obtain a better performance of a refractive index based SPR fibre sensor, the energy transferred to the PM is required to be extremely sensitive to the RI changes of the aqueous analyte [15]. When there are small RI changes in the analyte due to chemical/biochemical interactions, the real part of the  $n_{eff}$  of the PM should shift its position with respect to the light signal wavelength. As a consequence, the resonant wavelength occurring at the phase matching condition will also have a significant shift accordingly.

From Figs. 5 (a), we can observe only one single resonance peak for analyte RI ranges from 1.33 to 1.41 within the wavelength range from 0.5  $\mu\text{m}$  to 1.0  $\mu\text{m}$ . Here, the confinement loss increases as the RI of the analyte is increased. It should be noted that, due to the increasing high loss of the designed fibre and the existence of a secondary SPR caused by FM and hybrid PM in the longer wavelength, the loss peaks for RI=1.42 and 1.43 become more and more blunt and broad. As a result, the resonance peak can hardly be obtained and observed by using a spectrometer. Then, Fig. 5 (b) shows the trend for the family of the confinement loss curves of the analyte's RI in the range of 1.42 to 1.48 with dual resonance peaks in the wavelength bandwidth of 0.9  $\mu\text{m}$  from 0.9  $\mu\text{m}$  to 1.8  $\mu\text{m}$ . Due to the existence of SPR between fundamental core mode and hybrid surface plasmon, a sub-

peak is observed from the confinement loss spectra. As the secondary SPR always occurs at the longer wavelength, it is a 'plasmon-like' SPR with very high loss. In practical, because of the limitation on observation bandwidth of an optical spectrometer, we highly expect there would be only one single resonant peak for one analyte RI value. Therefore, in the detection process, dual-peaks characteristic will cause errors in the measurement within the certain sensing bandwidth. It is clear that the uniqueness and accuracy of single peak measurement cannot be guaranteed by the proposed sensor for RI of any analyte higher than 1.41 due to the overlap of two resonance peaks. This drawback limits the proposed sensor's detection range and sensing performance.

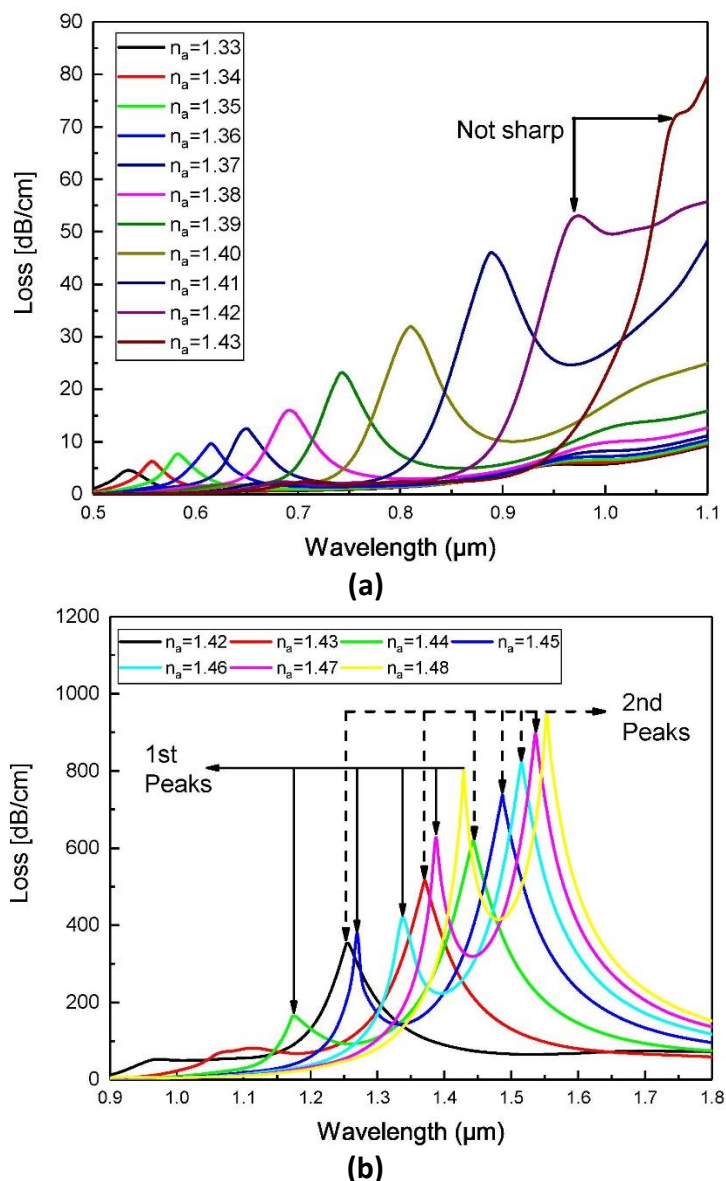


**Fig. 5.** The loss spectra for the analyte refractive index ( $n_a$ ) varying from (a) 1.33 to 1.43 in steps of 0.01 and (b) 1.42 to 1.48 in steps of 0.01

By introducing the wavelength interrogation method, the sensitivity of the sensor can be calculated in nm/RIU. For example, in Fig. 5 (a), the wavelength shifts between the confinement loss peaks for RI 1.40 and 1.41 is 79 nm. Hence, the sensitivity of the PCF-SPR sensor for the analyte RI change from 1.40 to 1.41 is calculated as 7900 nm/RIU.

## 5. Conclusion

In this paper, we have investigated a common D-shaped hexagonal photonic crystal for larger refractive index detection range. The numerical results show that the proposed sensor could achieve a maximum sensitivity of 7900 nm/RIU (RI =1.33 to 1.41), 5300 nm/RIU (RI =1.33 to 1.45) with thick analyte binding layer of 1500 nm and thin analyte binding layer of 500 nm, respectively. From the simulation results, we have observed that two different types of SPRs named as 'dielectric-like' SPR with low loss and 'plasmon-like' SPR with high loss. As the D-shaped hexagonal PCF-SPR sensor is one of the most promising and fabricable SPR sensors, we believe that it could be a potential sensing device for large range of analyte refractive index detection.

## References

- [1] Jorgenson, Ralph Corleissen, and Sinclair S. Yee. "Control of the dynamic range and sensitivity of a surface plasmon resonance based fiber optic sensor." *Sensors and Actuators A: Physical* 43, no. 1-3 (1994): 44-48.
- [2] Luan, Nannan, Ran Wang, Wenhua Lv, and Jianquan Yao. "Surface plasmon resonance sensor based on D-shaped microstructured optical fiber with hollow core." *Optics express* 23, no. 7 (2015): 8576-8582.
- [3] Hassani, Alireza, and Maksim Skorobogatiy. "Photonic crystal fiber-based plasmonic sensors for the detection of biolayer thickness." *JOSA B* 26, no. 8 (2009): 1550-1557.
- [4] Zhao, Yong, Ze-qun Deng, and Jin Li. "Photonic crystal fiber based surface plasmon resonance chemical sensors." *Sensors and Actuators B: Chemical* 202 (2014): 557-567.
- [5] Liu, Qi, and Qin Wang. "Refractive index sensor based on tapered PCF in-line interferometer." *Chinese Optics Letters* 10, no. 9 (2012): 090601-090601.
- [6] Sharma, Anuj K., and B. D. Gupta. "Fibre-optic sensor based on surface plasmon resonance with Ag–Au alloy nanoparticle films." *Nanotechnology* 17, no. 1 (2005): 124.
- [7] Suzuki, Hitoshi, Mitsunori Sugimoto, Yoshikazu Matsui, and Jun Kondoh. "Fundamental characteristics of a dual-colour fibre optic SPR sensor." *Measurement Science and Technology* 17, no. 6 (2006): 1547.
- [8] Bremer, Kort, and Bernhard Roth. "Fibre optic surface plasmon resonance sensor system designed for smartphones." *Optics express* 23, no. 13 (2015): 17179-17184.
- [9] Chu, Suoda, K. Nakkeeran, Abdosllam M. Abobaker, Sumeet S. Aphale, P. Ramesh Babu, and K. Senthilnathan. "Design and analysis of surface-plasmon-resonance-based photonic quasi-crystal fiber biosensor for high-refractive-index liquid analytes." *IEEE Journal of Selected Topics in Quantum Electronics* 25, no. 2 (2018): 1-9.
- [10] Leonard, Paul, Stephen Hearty, John Quinn, and Richard O'Kennedy. "A generic approach for the detection of whole *Listeria monocytogenes* cells in contaminated samples using surface plasmon resonance." *Biosensors and Bioelectronics* 19, no. 10 (2004): 1331-1335.
- [11] Monzón-Hernández, David, Joel Villatoro, Dimas Talavera, and Donato Luna-Moreno. "Optical-fiber surface-plasmon resonance sensor with multiple resonance peaks." *Applied optics* 43, no. 6 (2004): 1216-1220.
- [12] Shuai, Binbin, Li Xia, Yating Zhang, and Deming Liu. "A multi-core holey fiber based plasmonic sensor with large detection range and high linearity." *Optics express* 20, no. 6 (2012): 5974-5986.
- [13] Wang, Guangyao, Shuguang Li, Guowen An, Xinyu Wang, Yunyan Zhao, Wan Zhang, and Hailiang Chen. "Highly sensitive D-shaped photonic crystal fiber biological sensors based on surface plasmon resonance." *Optical and Quantum Electronics* 48, no. 1 (2016): 46.
- [14] An, Guowen, Shuguang Li, Xin Yan, Xuenan Zhang, Zhenyu Yuan, Haiyang Wang, Yanan Zhang, Xiaopeng Hao, Yaonan Shao, and Zhicong Han. "Extra-broad photonic crystal fiber refractive index sensor based on surface plasmon resonance." *Plasmonics* 12, no. 2 (2017): 465-471.
- [15] Lu, Hua, Xueming Liu, and Dong Mao. "Plasmonic analog of electromagnetically induced transparency in multi-nanoresonator-coupled waveguide systems." *Physical Review A* 85, no. 5 (2012): 053803.